PROCEEDINGS, 48th Workshop on Geothermal Reservoir Engineering
Stanford University, Stanford, California, February 6-8, 2023
SGP-TR-224

Characterizing Steam-Filled Fracture Zones at the Soda Lake Geothermal Field Using Seismic Double-Beam Neural Network (DBNN)

Yingcai Zheng[1], Hao Hu[1], Muhammad Nawaz Bugti[1], Jake Parsons[1], Lianjie Huang[2], Kai Gao[2], Trenton Cladouhos[3]

[1]Department of Earth and Atmospheric Sciences, University of Houston, TX 77204-5007, USA [2]Geophysics Group, Los Alamos National Laboratory, Los Alamos, NM 87545, USA [3]Formerly at Cyrq Energy, now at Stoneway Geothermal, Seattle, WA 98103

Yzheng12@uh.edu

Keywords: Geothermal, fracture characterization, fracture detection, machine learning, small-scale fractures, double beam, DBNN

ABSTRACT

Previous geological studies in the Basin and Range of the Western U.S. have shown that conventional geothermal systems are usually located in geological settings of intense fracturing. The field studied here, Soda Lake geothermal field is one of the first geothermal fields developed in Nevada. The field contains steam vents and warm ground. However, most of the recent geothermal developments have been blind, with no surface hot springs or steam, and future developments are also likely to be blind. Therefore, characterizing subsurface fractures may provide an approach to unraveling blind geothermal systems. The sizes of small-scale fractures are much smaller than the seismic wavelength. Therefore, seismic migration cannot directly image small-scale fractures. We have demonstrated that our seismic double-beam (DB) method is effective in characterizing the fracture parameters in synthetic data: fracture orientation, density, and compliance. Augmented by a machine learning algorithm, our new double beam neural network (DBNN) algorithm can predict the locations and orientations of discrete fractures. We apply our DBNN method to the 3D Soda Lake seismic data to identify additional blind geothermal resources, particularly the shallow steam-charged fracture zones with large fracture compliance values. We identify four possible drilling targets showing high fracture compliance values, with one of them (Well 41-33) previously verified as a hot steam zone via drilling. Our seismic results on fractures and faults, in addition to known geology, well-logging information, and production data, can be used to identify new drilling targets.

1. INTRODUCTION

Faults and fractures have been shown to play important roles in controlling the geothermal systems in the Great Basin in the west U.S. (Faulds and Hinz, 2015). Better characterization of subsurface faults/fractures can allow us to develop new resources and to extend the life of existing geothermal power plants.

We distinguish small-scale fractures (smaller than the dominant wavelength) from faults (larger than the dominant wavelength with possible slip on the fault surface). In this paper, we focus on seismic characterization of subsurface small-scale fractures using the double-beam neural network (DBNN) method (Zheng *et al.*, 2021c) at the Soda Lake geothermal field. We do not discuss how to image faults but refer readers to other related works (Gao *et al.*, 2021a; Gao *et al.*, 2021b; Gao *et al.*, 2021c; Gao *et al.*, 2022; Huang *et al.*, 2023).

Traditionally, fractures are characterized using the effective medium theory in which aligned fractures in rocks can cause anisotropy (e.g., Thomsen, 1995). Amplitude-versus-angle/azimuth (AVAz) for reflected waves (e.g., Rüger and Tsvankin, 1997; Lynn *et al.*, 1999; Perez *et al.*, 1999; Thomsen, 1999; Vasconcelos and Grechka, 2007) and shear-wave splitting (e.g., Crampin, 1985; Tatham *et al.*, 1992; Vetri *et al.*, 2003; Long, 2013; Verdon and Wustefeld, 2013) are commonly used to indirectly infer fracture properties. However, fractures (or joints) usually appear in clusters (Gale *et al.*, 2007). Because of the random distribution, the fracture system can exhibit multiple spatial scales (e.g., distance between neighboring fractures, sizes of the fracture clusters, distance between clusters, etc.). Because of multiple scattering and interference, the effective-medium methods can produce erroneous results for randomly distributed fractures (Fang *et al.*, 2017). Another weakness of the anisotropy-based method is that it is challenging to handle thin fractured layers. Can we see small-scale fractures in seismic migration? Using a 3D synthetic example based on the Soda Lake geothermal field, Zheng *et al.* (2021c) showed that it is not likely to be able directly image small-scale fractures because the fracture scattering energy is extremely weak compared with reflections from geological formations. There are no image offsets across the fracture interface so conventional fault detection algorithms cannot detect fractures.

In this paper, we consider imaging small-scale fractures using a neural network architecture that augments the double-beam (DB) method (Zheng *et al.*, 2013; Hu and Zheng, 2018; Hu *et al.*, 2018). The method is called double-bean neural network (DBNN) method (Zheng *et al.*, 2021c). Intuitively, the method works in the following manner. We partition the subsurface into many fracture target 'boxes.' We select a box that may contain zero or multiple fracture sets. We synthesize point sources on the surface as directional source beams (Ding *et al.*, 2017; Ding *et al.*, 2019) to shoot seismic-wave energy into the box and analyze the interference pattern of the scattered/reflected beam at receivers. This interference pattern contains subsurface fracture parameters: fracture orientation, density, and fracture compliance (Schoenberg, 1980; Schoenberg and Sayers, 1995).We recently developed a DBNN method to interpret the DB interference patterns as discrete fracture networks (DFNs) (Li *et al.*, 2019; Zheng *et al.*, 2021c). The DBNN can automatically and accurately invert the DFNs from surface-recorded active seismic data. We recently validated the DBNN method using 3D synthetic seismic data based on the Soda

Lake geological and geophysical models (Zheng *et al.*, 2021c). The goal of this paper is applying the DBNN to the Soda Lake field data to detect steam charged fracture zones.

We organize the paper as follows. First, we briefly review the DBNN method. We then describe the Soda Lake seismic survey and the seismic dataset. Finally, we apply our DBNN to this dataset to detect shallow steam zones above the basalt body.

2. METHODS

We briefly review the method for extracting DB interference (DBI) patterns from surface-recorded active seismic data, and then describe how to train the DBNN and use the well-trained DBNN to *transform* DBI into DFNs.

2.1 DBI Pattern

The DB method characterizes subsurface fractures using a source-beam and a receiver-beam (Figure 1a) (Zheng *et al.*, 2013; Hu and Zheng, 2018; Hu *et al.*, 2018; Hu *et al.*, 2021). The principle of the DB method is seeking the spatial scattering interference pattern, $\sigma(\varphi, a|\omega)$, based on multiple scattering of a local incident plane wave upon a set of fractures The interference pattern is a complex-valued double-beam interference (DBI) pattern (Figure 1b). The parameters φ, a, ω, are the fracture orientation, fracture spacing, and the angular frequency of the seismic wave, respectively. Fracture planes are assumed vertical, and it is a valid assumption if the maximum stress is along the vertical direction. Within each fracture target (i.e., "box"), we search all possible (φ, a) using all possible source-receiver beams and obtain $\sigma(\varphi, a|\omega)$ for the fracture target location using multiple frequencies. At the true values (φ, a), the modulus $|\sigma(\varphi, a)|$ corresponds to high-amplitude "bright spots" (Figure 1b). Importantly, the amplitudes of the bright spots are proportional to the average fracture compliance values for that particular fracture set in the "box." Multiple co-existent fracture sets in the same box can also be detected using DB. Based on the DBI, we can identify the existence of fractures if there are "bright spots." In addition, we can also infer the fracture spacing, orientation, and relative compliance according to the location and amplitude of "bright spots" for each subsurface target. Such interpretations of DBI were mainly performed by human previously. Large compliance values indicate presence of gas or steam.

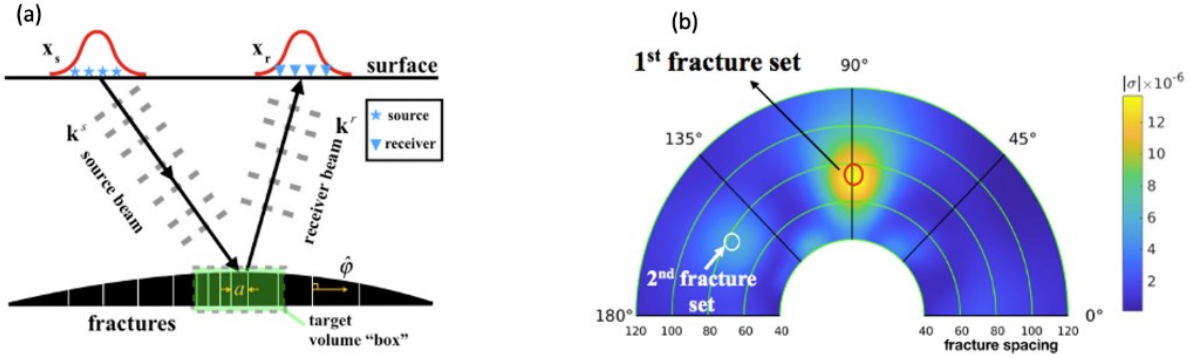

Figure 1: Schematic diagram of the DB fracture characterization method. (a) Stars and triangles represent sources and receivers, respectively. Parameter a is the local fracture spacing in the target region. Parameter φ is the fracture normal direction. (b) An example of the absolute value of the complex-valued DBI pattern, $|\sigma(\varphi, a)|$. Two picked bright spots show two fracture sets. Radial direction indicates fracture spacing a. The polar angle is the fracture orientation φ. The magnitude of $|\sigma(\varphi, a)|$ at the bright spot indicates the fracture compliance for this set of fractures around the target.

2.2 DBNN – Interpreting DBI as DFN Using Neural Networks

Automatically converting the DBI pattern to the DFN map using neural networks is an image-to-image transform. Li *et al.* (2019) and Zheng *et al.* (2021b); (Zheng *et al.*, 2021c) described this algorithm in detail. They used a fully connected neural network to automatically convert a DBI to a DFN for each subsurface target. Under ideal acquisition conditions, DBI and DFN can be considered as Fourier transform pairs. Hence, DBNN is physics-guided machine learning but for an imperfect data acquisition configuration. Using 3D synthetic data based on the Soda Lake field geometry, Zheng *et al.* (2021c) demonstrated that DBNN correctly inverts for DFNs from synthetic DBIs.

3. RESULTS — STEAM ZONE CHARACTERIZATION AT THE SODA LAKE GEOTHERMAL FIELD

The Soda Lake 3D seismic dataset was described by Gao *et al.* (2021a). The entire 3D seismic acquisition covered a rectangle region with a size of 6 km by 6 km (see the acquisition geometry in Figure 2). There are 8,371 shots and 2,972 receivers. The entire seismic dataset contains about 5 million traces. Each trace has 2,001 samples with a sampling interval of 2 ms (see a seismic gather in Figure 3).

The Soda Lake geothermal field has been in production since 1972 (Benoit, 2016; McLachlan, 2018). A distinct geological feature in the field is the basaltic body at a depth about ~500 m. There is a significant interest for exploration of new heat sources above the basalt. The most prolific producing well at Soda Lake is Well# 41-33 (Figure 4) that produces hot water (370 °F) and steam at a depth of 815 feet (or 248 m). There is a great need to use seismic data to find additional resources and discriminate permeable and impermeable zones where traditional seismic workflows cannot (Benoit, 2016).

We focus on targets at shallow depths above the basaltic unit where fractures may not be pervasively present. The main geothermal targets are steam-charged localized fracture zones. For locating the shallow fracture targets above the basalt body, we use DBNN to detect possible fractures around two depths, 250 m, and 300 m.

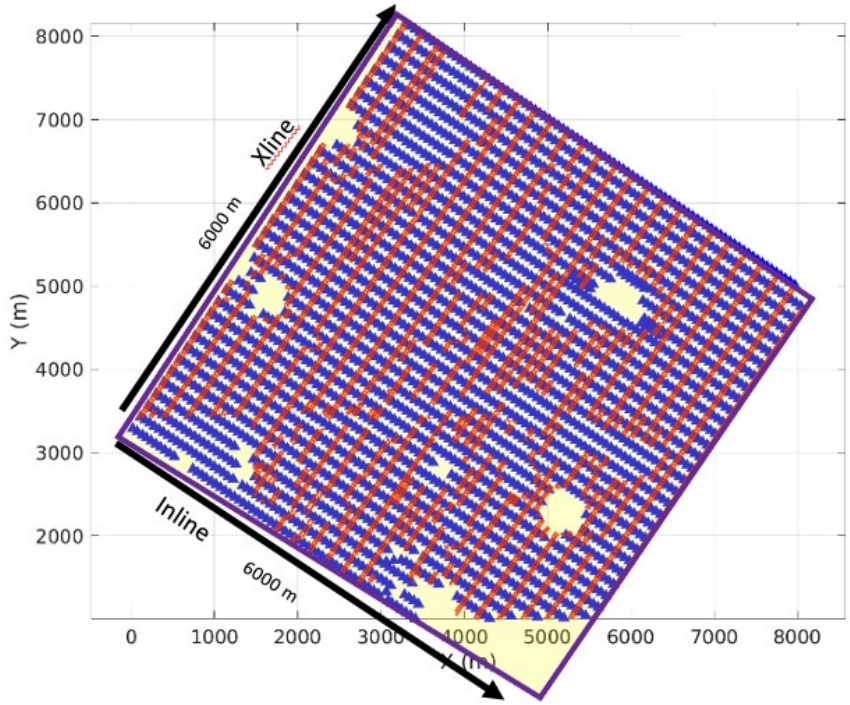

Figure 2: The geometry of the Soda Lake field seismic acquisition showing sources (red) and geophones (blue).

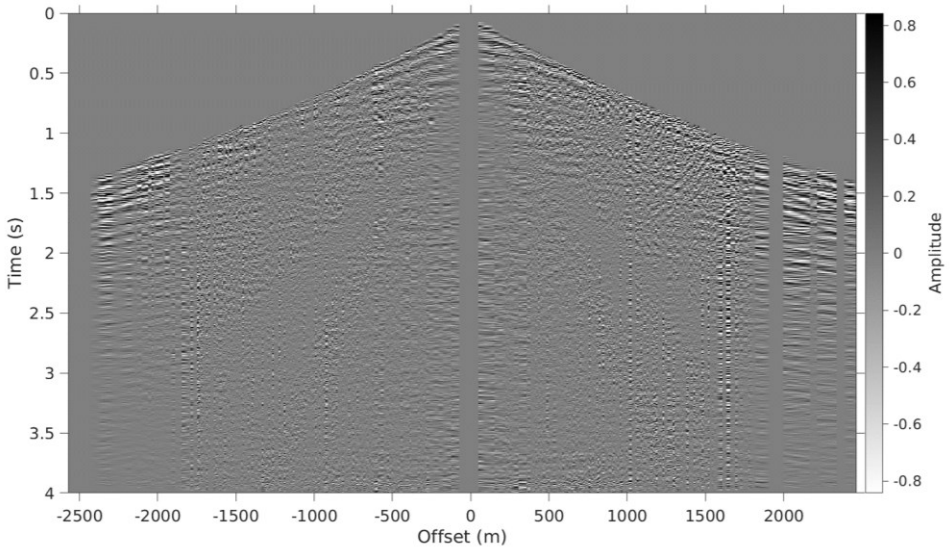

Figure 3: Sample seismic shot gather of the Soda Lake field seismic data. The maximum offset is about 2600 m. The recording time is 4 s at a sampling interval of 2 ms. (From Zheng et al. (2021a))

To reveal the fracture distribution in the entire region covered by the seismic acquisition, we use 41x41 targets (i.e. boxes in horizontal directions) regularly, spaced at a spacing of 100 m by 100 m at two depths: 250 m and 300 m. We use three frequencies, 40 Hz, 50 Hz, and 60 Hz for DBNN. True fractures appear in all the three frequencies. Therefore, multiple frequency implementation of DBNN provides a self-validation means.

We show the inverted fracture compliance maps at two depths (250 m and 300 m) in Figure 5a and b, respectively. The inset rose diagrams show fracture orientations for all 441 fracture targets. We identified four locations (P0, P1, P2, P3, and P4 in Figure 5a &b) showing large fracture compliance values. We call them steam prospects. Steam-charged localized fracture zone should have large fracture compliance values, which measures how easy the fracture can be deformed by a given stress (compressional or shear). Steam-charged zones are more deformable than liquid saturated zones. P0 is very close to well 41-33 at depth 250 m. Well 41-33 has been verified to produce hot water and steam. We hypothesize that the other prospects, P1, P2, and P3, could also be the steam-charged fracture zones.

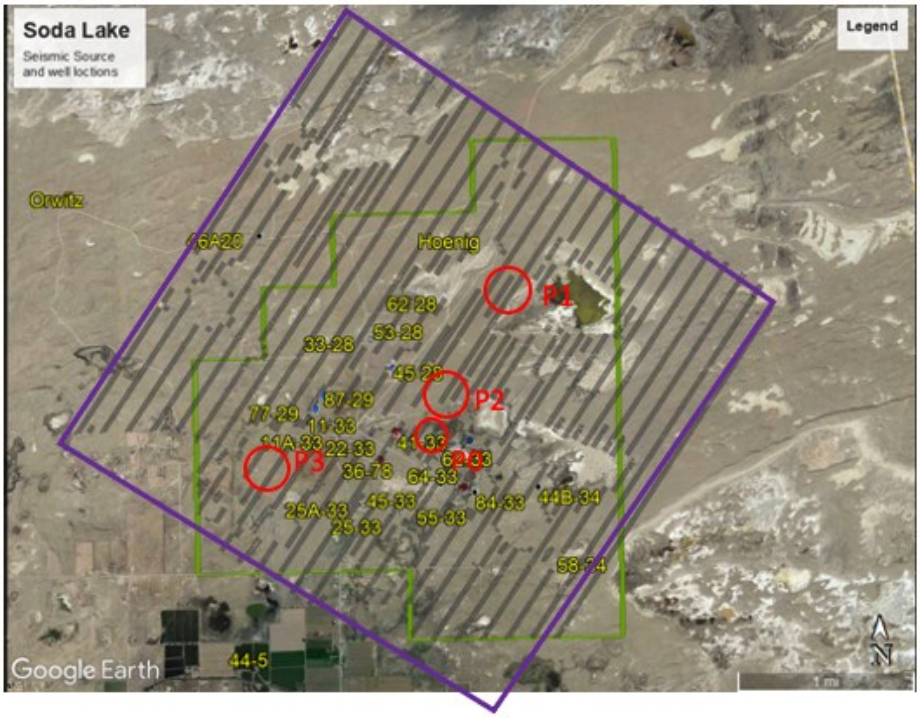

Figure 4: Well locations (yellow) superimposed on the seismic acquisition geometry. The purple square shows the seismic acquisition boundary. The circles, P0, P1, P2, and P3 are proposed prospects (see Figure 5).

4. DISCUSSION

To make predictions based only one type of data (seismic in this case) could carry much uncertainty. However, it is encouraging to see one of the four proposed prospects, P0, corresponds to the previously drilled Well 41-33 that produces hot water/steam. Future work is needed to refine the results. First, we can reduce the beam width (currently 200m) and the size of the interrogation box (now 100 m by 100 m) to achieve a higher spatial resolution. Secondly, P3 is at the edge of the DBNN scanned region. We can enlarge the DBNN scanning region. Thirdly, we can use elastic DB, in particular the P to S converted waves, to characterize the steam zones. S waves could have better sensitivities to steam. Finally, we need to integrate more field data such as geology information and well logging to make better predictions.

5. CONCLUSIONS

We have characterized subsurface small-scale fractures at the Soda Lake geothermal field using our double-beam neural network (DBNN) method and the 3D surface seismic data. We have focused on the shallow regions above the basalt body. Our DBNN results in three different frequency bands (40Hz, 50 Hz, and 60 Hz) produce consistent fracture results. At 250 m depth, we have found four high fracture compliance regions (P0-P3) that could be prospects to be further evaluated for hot water/steam drilling. Three (P0, P1, P3) of the four prospects seem to be present down to about 300 m in depth. These results are encouraging. Prospect P0 is close to the previously drilled Well 41-33 that is the best producer in the region. Our method is different from the traditional seismic workflow and can be a useful tool for siting new wells to increase geothermal production.

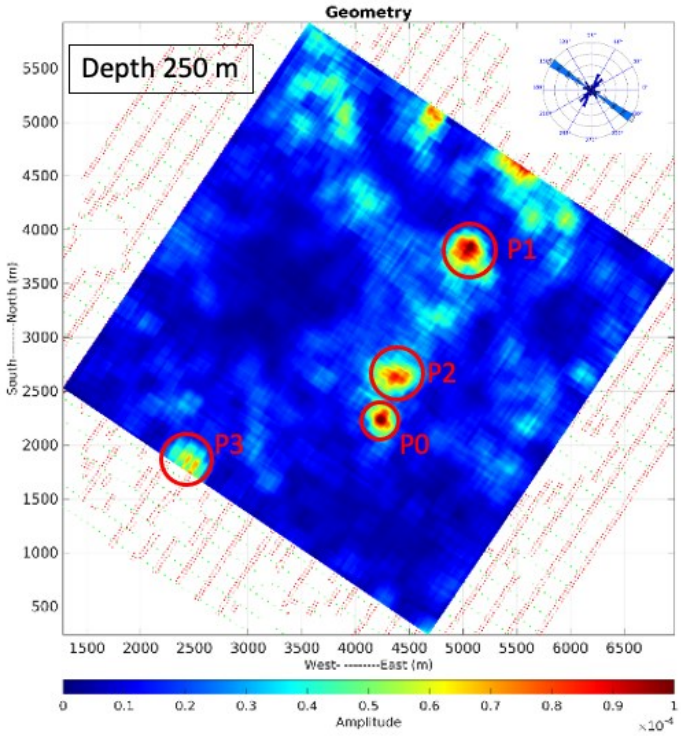

(a)

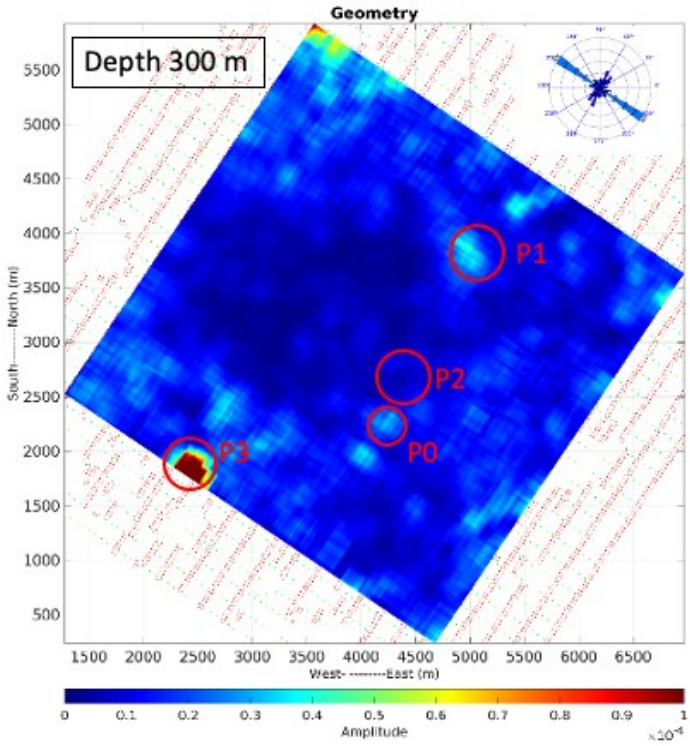

(b)

Figure 5: Inverted fracture maps at two different depths (a) 250 m and (b) 300 m. The blue region in both (a) and (b) are the DBNN scanned region. High compliance prospect regions are labeled as P0, P1, P2, and P3.

ACKNOWLEDGMENTS

This work was supported by the U.S. Department of Energy (DOE) Geothermal Technologies Office with funding No. DE-EE0008764, a joint project between the University of Houston and Los Alamos National Laboratory (LANL). LANL is operated by Triad National Security, LLC, for the U.S. DOE National Nuclear Security Administration (NNSA) under Contract No. 89233218CNA000001. We thank Cyrq Energy for providing the Soda Lake 3D surface seismic data. This research used computing resources provided by the LANL Institutional Computing Program supported by the U.S. DOE NNSA under Contract No. 89233218CNA000001. We also used computing facilities provided by the UHXfrac group at the University of Houston.

REFERENCES

Benoit, D. (2016), Soda Lake Geothermal Field Case History 1972 to 2016, *GRC Transactions*, **40**, 523-534,

Crampin, S. (1985), Evaluation of Anisotropy by Shear-Wave Splitting, *Geophysics*, ***50***(1), 142-152.

Ding, Y., Y. Zheng, H.-W. Zhou, M. Howell, H. Hu, and Y. Zhang (2017), Propagation of Gaussian wave packets in complex media and application to fracture characterization, *Geophys. J. Int.*, ***210***(2), 1244-1251.

Ding, Y., H.-W. Zhou, Y. Zheng, and Y. Wo (2019), Synthesis of Directional Wave Packets from Shot Records, *Pure Appl. Geophys.*, ***176***(10), 4321-4333.

Fang, X., Y. Zheng, and M. Fehler (2017), Fracture clustering effect on amplitude variation with offset and azimuth analyses, *Geophysics*, ***82***(1), N13-N25.

Faulds, J., and N. Hinz (2015), Favorable tectonic and structural settings of geothermal systems in the Great Basin region, western USA: Proxies for discovering blind geothermal systems, *Proceedings World Geothermal Congress 2015* Melbourne, Australia, 19-25 April 2015

Gale, J. F. W., R. M. Reed, and J. Holder (2007), Natural fractures in the Barnett Shale and their importance for hydraulic fracture treatments, *Aapg Bulletin*, ***91***(4), 603-622.

Gao, K., L. Huang, and T. Cladouhos (2021a), Three-dimensional seismic characterization and imaging of the Soda Lake geothermal field, *Geothermics*, ***90***, 101996.

Gao, K., L. Huang, R. Lin, H. Hu, Y. Zheng, and T. Cladohous (2021b), Delineating Faults at the Soda Lake Geothermal Field Using Machine Learning, *PROCEEDINGS, 46th Workshop on Geothermal Reservoir Engineering*, SGP-TR-216, Stanford University, Stanford, California

Gao, K., L. Huang, and Y. Zheng (2022), Fault Detection on Seismic Structural Images Using a Nested Residual U-Net, *IEEE Transactions on Geoscience and Remote Sensing*, ***60***, 1-15.

Gao, K., L. Huang, Y. Zheng, R. Lin, H. Hu, and T. Cladohous (2021c), Automatic fault detection on seismic images using a multiscale attention convolutional neural network, *Geophysics*, ***87***(1), N13-N29.

Hu, H., A. Alali, A. Almomin, and Y. Zheng (2021), 3D seismic characterization of fractures using elastic P-to-S double beams, *Geophysics*, R927-R937.

Hu, H., and Y. Zheng (2018), 3D seismic characterization of fractures in a dipping layer using the double-beam method, *Geophysics*, ***83***(2), V123-V134.

Hu, H., Y. Zheng, X. Fang, and M. C. Fehler (2018), 3D seismic characterization of fractures with random spacing using the double-beam method, *Geophysics*, ***83***(5), M63-M74.

Huang, L., K. Gao, D. Li, Y. Zheng, and T. Cladouhos (2023), Delineating Faults beneath Basalt at the Soda Lake Geothermal Field, *PROCEEDINGS, 48th Workshop on Geothermal Reservoir Engineering*, Stanford University, Stanford, California, February 6-8, 2023. SGP-TR-224. pp.8.

Li, J., H. Hu, and Y. Zheng(2019), Physics-guided machine learning identification of discrete fractures from double beam images, *SEG, Expanded abstracts*, San Antonio,

Long, M. D. (2013), Constraints on subduction geodynamics from seismic anisotropy, *Rev Geophys*, ***51***(1), 76-112.

Lynn, H. B., W. E. Beckham, K. M. Simon, C. R. Bates, M. Layman, and M. Jones (1999), P-wave and S-wave azimuthal anisotropy at a naturally fractured gas reservoir, Bluebell-Altamont Field, Utah, *Geophysics*, ***64***(4), 1312-1328.

McLachlan, H. S. (2018), Stratigraphy, Structure, and Fluid Flow at the Soda Lake Geothermal Field, western Nevada, USA, Ph.D., 281 pp, University of Nevada Reno.

Perez, M. A., R. L. Gibson, and M. N. Toksoz (1999), Detection of fracture orientation using azimuthal variation of P-wave AVO responses, *Geophysics*, ***64***(4), 1253-1265.

Rüger, A., and I. Tsvankin (1997), Using AVO for fracture detection: Analytic basis and practical solutions, *The Leading Edge*, ***16***(10), 1429-1434.

Schoenberg, M. (1980), Elastic wave behavior across linear slip interfaces, *Journal of the Acoustical Society of America*, ***68***(5), 1516-1521.

Schoenberg, M., and C. M. Sayers (1995), Seismic anisotropy of fractured rock, *Geophysics*, ***60***(1), 204-211.

Tatham, R. H., M. D. Matthews, K. K. Sekharan, C. J. Wade, and L. M. Liro (1992), A Physical Model Study of Shear-Wave Splitting and Fracture Intensity, *Geophysics*, ***57***(4), 647-652.

Thomsen, L. (1995), Elastic anisotropy due to aligned cracks in porous rock, *Geophysical Prospecting*, ***43***(6), 805-829.

Thomsen, L. (1999), Converted-wave reflection seismology over inhomogeneous, anisotropic media, *Geophysics*, ***64***(3), 678-690.

Vasconcelos, I., and V. Grechka (2007), Seismic characterization of multiple fracture sets at Rulison Field, Colorado, *Geophysics*, ***72***(2), B19-B30.

Verdon, J. P., and A. Wustefeld (2013), Measurement of the normal/tangential fracture compliance ratio (ZN/ZT) during hydraulic fracture stimulation using S-wave splitting data, *Geophys Prospect*, ***61***, 461-475.

Vetri, L., E. Loinger, J. Gaiser, A. Grandi, and H. Lynn (2003), 3D/4C Emilio: Azimuth processing and anisotropy analysis in a fractured carbonate reservoir, *The Leading Edge*, ***22***(7), 675-679.

Zheng, Y., J. Li, H. Hu, K. Gao, L. Huang, and T. Cladouhos (2021a), Seismic Double-beam Neural Network Approach to Characterizing Small-Scale Fractures in Geothermal Fields, *GRC Transactions*, **45**, 1358-1368,

Zheng, Y., J. Li, R. Lin, H. Hu, K. Gao, and L. Huang (2021b), Physics-Guided Machine Learning Approach to Characterizing Small-Scale Fractures in Geothermal Fields, *46th Workshop on Geothermal Reservoir Engineering*, Stanford

Zheng, Y., J. Li, R. Lin, H. Hu, K. Gao, and L. Huang (2021c), Physics-Guided Machine Learning Approach to Characterizing Small-Scale Fractures in Geothermal Fields *PROCEEDINGS, 46th Workshop on Geothermal Reservoir Engineering*, Stanford University, Stanford, California, February 15-17, 2021. SGP-TR-218. pp.9.

Zheng, Y. C., X. D. Fang, M. C. Fehler, and D. R. Burns (2013), Seismic characterization of fractured reservoirs by focusing Gaussian beams, *Geophysics*, ***78***(4), A23-A28.